

# Pressure-induced magnetic and electronic transitions in the layered Mott insulator $\text{FeI}_2$

M. P. Pasternak,\* W. M. Xu, and G. Kh. Rozenberg  
*School of Physics and Astronomy, Tel Aviv University, 69978 Tel Aviv, Israel*

R. D. Taylor  
*MST-10, MS-K764, Los Alamos National Laboratory, Los Alamos, New Mexico 87545*

G. R. Hearne  
*Department of Physics, University of the Witwatersrand, P O Wits 2050, Johannesburg-Gauteng, South Africa*

E. Sterer  
*Nuclear Research Center-Negev, P.O. Box 9001, Beer-Sheva, Israel*  
 (Received 13 August 2001; published 13 December 2001)

Powder x-ray diffraction, electrical resistance, and  $^{57}\text{Fe}$  Mössbauer spectroscopy at pressures to at least 40 GPa in diamond anvil cells have been employed to investigate the pressure evolution of the structural, electrical-transport, and magnetic properties of the antiferromagnetic insulator  $\text{FeI}_2$ . Up to 18 GPa, the volume decreases by 25%, the resistivity decreases by eight orders of magnitude,  $T_N$  increases 16-fold to 150 K, and the  $\text{Fe}^{2+}$  moments remain parallel to the  $c$  axis. The change in the isomer shift (IS), which is *negatively* proportional to the change in the  $s$ -electron density at the Fe nucleus, follows the volume reduction by continuously decreasing from 1.0 to 0.8 mm/s, the quadrupole splitting (QS) increases monotonically from 0.6 mm, peaking at 0.85 mm/s by 12 GPa, and decreases to 0.75 at 18 GPa, and the magnetic hyperfine field  $H_{\text{hf}}$  composed of *spin* and *orbital* terms with opposite signs increases from 8 to 12 T. At  $\sim 18$  GPa the *orbital term* quenches, as is evident from a Mössbauer component characterized by  $H_{\text{hf}}=32$  T and  $e^2q_{zz}Q(3\cos^2\theta-1)=0$ , where the moments tilt to  $55^\circ$ , and  $T_N$  increases to 260 K. At 20 GPa an isostructural first-order phase transition occurs, accompanied by a discontinuous  $\sim 5\%$  decrease in volume and a considerably lower QS and IS. The  $c$  axis decreases by 5% with no decrease in the  $a$  axis, suggesting a considerable contraction of the Fe-I bond lengths. The high-pressure phase (HP) is diamagnetic, as characterized by a pure quadrupole-split spectrum to the lowest temperature of 5 K. The abundance of this diamagnetic phase increases with rising pressure reaching 100% by  $\sim 38$  GPa. The HP phase is also metallic, as shown by  $R(P,T)$  data. The observation of diamagnetism, metallic behavior, and the considerable reduction in volume distances establishes that a *Mott* or *charge-transfer* transition has occurred, resulting in the total collapse of any electron correlation. The coexistence of several phases and their respective abundances were determined from the Mössbauer data.

DOI: 10.1103/PhysRevB.65.035106

PACS number(s): 62.50.+p, 61.10.-i, 71.30.+h, 76.80.+y

## I. INTRODUCTION

Pressure-induced closure of an electron-correlation gap, resulting in an associated Mott insulator-metal transition,<sup>1</sup> received experimental corroboration for the first time in a combination of magnetic, electrical-transport, and structural studies in  $\text{NiI}_2$ ,<sup>2</sup> and later in  $\text{CoI}_2$ .<sup>3</sup> Considering the experimental fact that magnetic properties at  $P > \sim 10$  GPa can be readily probed only by Mössbauer spectroscopy (MS),<sup>4</sup> those high-pressure studies were carried out with  $^{129}\text{I}$  MS. This played a crucial role in probing the magnetic properties at the cation site via the *transferred* hyperfine interaction (THI). The main disadvantage of the THI method, however, is its inability to probe directly the more subtle magnetic-electronic properties of the transition-metal (TM) ion itself such as, a *high-spin* $\rightarrow$ *low-spin* crossover, the role of orbital-vs spin-term contributions to the TM magnetic moment, changes in local density as measured by the isomer shift (IS), etc. At ambient pressure  $\text{FeI}_2$  is classified as a Mott insulator that, by virtue of its strong on-site electron-electron correlation within the  $d$  bands, has a localized moment, becomes antiferromagnetic below  $T_N=9.3$  K (Ref. 5) (its Néel

temperature), and is an insulator with a large optical gap that persists at temperatures far above  $T_N$ .

Iron di-iodide crystallizes in the hexagonal  $\text{Cd}(\text{OH})_2$  structure [space group  $C\bar{3}m$ ],<sup>6</sup> a crystal structure at ambient pressure similar to that of  $\text{NiI}_2$ ,  $\text{FeCl}_2$ , and other TM halides.  $\text{FeI}_2$  is a layered compound having a sheet of Fe atoms alternating with double layers of iodine atoms along the  $c$  axis (see Fig. 1). However, the spin arrangement is complex,<sup>7</sup> and differs from other antiferromagnetic halides. As for  $^{57}\text{Fe}$  MS studies, an atomic scale magnetic probe, the relevant information is that the moments are parallel or antiparallel to the  $c$  axis at low pressures. The principal part of the crystal field around  $\text{Fe}^{2+}$  is of cubic symmetry, but in addition there is a crystal field of trigonal symmetry that arises from the non-cubic arrangement of cations.<sup>8,9</sup> Because of its anisotropic layer structure, the component of the orbital angular momentum along the trigonal axis ( $c$  axis) is not quenched.<sup>10,11</sup>

Early  $^{57}\text{Fe}$  Mössbauer studies carried out to 35 GPa by Hearne *et al.*<sup>12</sup> revealed a drastic change of the magnetic hyperfine field ( $H_{\text{hf}}$ ) around 20 GPa, suggesting a phase transition. However, the quality of these early MS-DAC experiments and the limited pressure achieved was inadequate

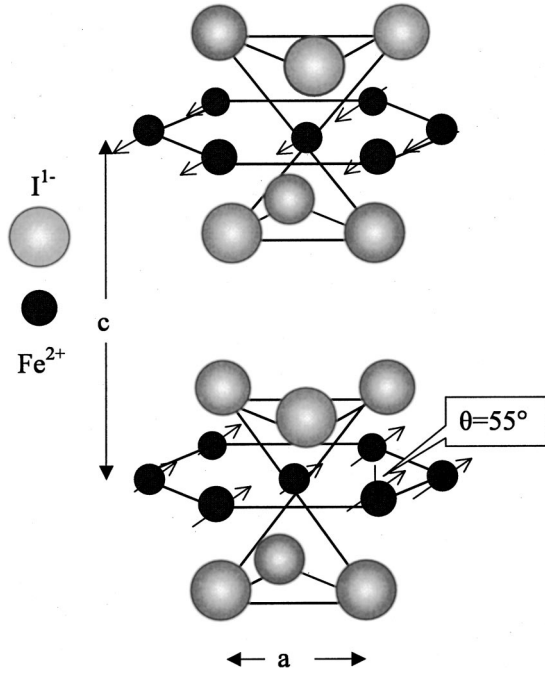


FIG. 1. The crystal structure of antiferromagnetic  $\text{FeI}_2$  at ambient pressure. The crystal is formed of I-Fe-I layers, that are covalently bonded and separated by typical I-I van der Waal's distances. ( $T_N=9.3$  K). In the 18–30-GPa range as a result of  $\text{Fe}^{2+}$  orbital quenching the moments in each layer are *ferromagnetically coupled* within each Fe-Fe plane, and are oriented at angles of  $55^\circ$  and  $235^\circ$  with respect to  $c$  axis. Successive Fe layers are antiferromagnetically coupled.

to draw firm conclusions as to the nature of the magnetism and the cause of the changes in  $H_{\text{hf}}$ . Conventional x-ray diffraction (XRD) performed by Sterer<sup>13</sup> were not accurate enough to ascertain any crystallographic phase transition in this pressure range. In the present work we have combined the methods of  $^{57}\text{Fe}$  MS, x-ray powder diffraction using a synchrotron source in the angle-dispersive mode, and electrical resistance measurements, up to 50 GPa, to study the evolution of magnetic, electronic, and structural details in  $\text{FeI}_2$ . The considerably improved quality of the Mössbauer and the XRD data, combined with electrical measurements, permit a rather precise interpretation and consistent understanding of the progressive changes in the magnetic/electronic properties with pressure and the assessment and classification of the collapse of the correlated state, i.e., the Mott transition, in  $\text{FeI}_2$ .

## II. EXPERIMENT

Samples of  $\text{FeI}_2$  were prepared in milligram quantities by metal-vapor reaction of the elements in an evacuated quartz tube.<sup>14</sup> For Mössbauer studies,  $\text{FeI}_2$  isotopically enriched to 20%  $^{57}\text{Fe}$  was prepared. Due to the extreme hygroscopic nature of  $\text{FeI}_2$  the crimson-red flakes were loaded in a glove box under exceptionally dry conditions into miniature opposing-plates DACs,<sup>15</sup> developed and built at Tel Aviv University. Initial dimensions of the sample cavities in the Re gasket were  $250 \times 35$ - $\mu\text{m}$  for  $P < 30$  GPa and 150

$\times 35$   $\mu\text{m}$  for  $P > 30$  GPa. Argon was used as a pressure medium for MS and XRD studies, and no medium was used for the resistance measurements. Pressure was determined by the ruby fluorescence method.<sup>16</sup> The pressure gradients in the samples were about 5% in the pressure range of 1–20 GPa, and perhaps 10% above 30 GPa.

*Mössbauer measurements* were carried out in a top-loaded LHe cryostat in the 5–300-K temperature range up to  $\sim 50$  GPa using a  $^{57}\text{Co}(\text{Rh})$  point source. Typically about 24 h was required for each Mössbauer spectrum.

*Resistance measurements* were performed to 44 GPa using a quasi-four-probe method. Gold wire electrodes 10  $\mu\text{m}$  in diameter were placed on the truncated culet of one of the anvils insulated from the metallic gasket by an insulating layer mixture of  $\text{Al}_2\text{O}_3$  and NaCl. At each pressure measurements were carried out as function of temperature down to 4.2 K by lowering the sample, in a controlled manner, into a LHe storage Dewar.

*X-ray-diffraction* studies were performed at 300 K up to 66 GPa in the angle-dispersive mode at the ID30 beamline of the *European Synchrotron Radiation Facility*. Diffraction images were collected at a wavelength  $\lambda = 0.4246$  Å using image plates with exposure times at each pressure of  $\sim 5$  min. The image data were integrated using the FIT2D program,<sup>17</sup> and the resulting diffraction patterns were analyzed by the GSAS<sup>18</sup> and PEAKFIT 4.0 programs.

## III. RESULTS

### A. Mössbauer studies

Typical Mössbauer spectra at 5 K ( $T \ll T_N$ ) showing the different phases evolving with increasing pressure are presented in Fig. 2. Up to  $\sim 18$  GPa, designated as the low pressure (LP1) phase, the quadrupole interaction is comparable in strength to the magnetic interaction, and the following *spin Hamiltonian*  $H$  governing the nuclear excited ( $I^* = \frac{3}{2}$ ) and ground ( $I = \frac{1}{2}$ ) states of the 14.4-keV level in  $^{57}\text{Fe}$  was utilized to fit the experimental results:

$$\begin{aligned}
 H(I^*) &= -\mu^*(I_z/I^*)H_{\text{hf}}(\theta) \\
 &+ \frac{e^2q_{zz}Q}{4I^*(2I^*-1)}[3I_z^2 - I^*(I^*+1)], \\
 H(I) &= -\mu(I_z/I)H_{\text{hf}}, \quad (1)
 \end{aligned}$$

where  $\mu$  and  $\mu^*$  are the ground and excited-state nuclear moments, respectively,  $\theta$  is the angle formed between  $H_{\text{hf}}$  and the electric-field gradient  $eq_{zz}$ , and  $e^2q_{zz}Q$  is the quadrupole coupling.<sup>19</sup> A spectrum typical of the 0–15-GPa pressure range is shown in Fig. 2(a). The solid line through the experimental points is a theoretical fit using Eqs. (1). Characteristic values at  $\sim 5$  K of  $H_{\text{hf}}$ ,  $e^2q_{zz}Q/2$ , IS, and  $\theta$  corresponding to the LP1 phase are 10 T,  $\pm 1.4$ –0.7 mm/s, +0.9 mm/s, and  $0^\circ$ , respectively. Since  $eq_{zz}$  coincides with the  $c$  axis (see Fig. 1) this fit with  $\theta = 0^\circ$  says that the magnetic moment also lies along the  $c$  axis, consistent with neutron diffraction measurements at ambient pressure.<sup>7</sup>

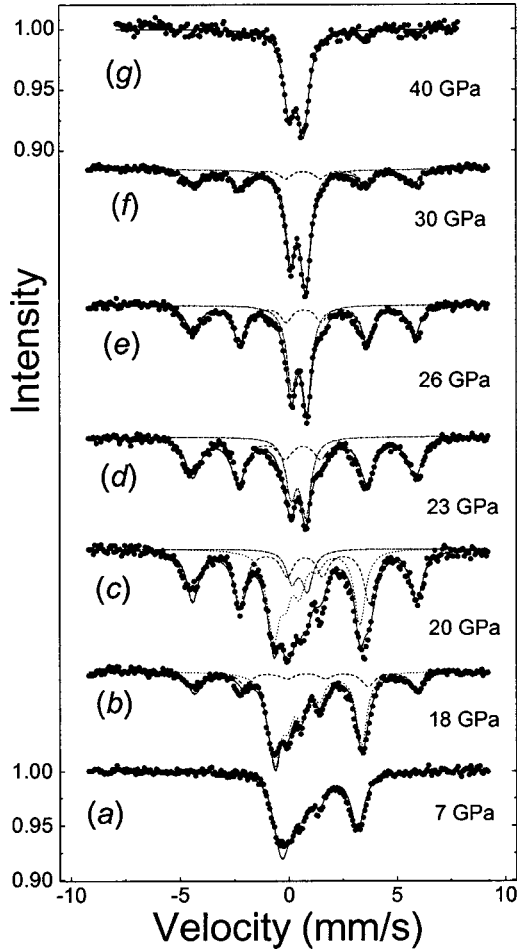


FIG. 2. Evolution of the Mössbauer spectra recorded at 5 K, depicting the pressure-induced phases. (a) Spectra typical of the LP1 phase in which  $H_{\text{hf}}$  is composed primarily of spin and orbital terms with opposing signs (see the text). In this pressure regime, up to 18 GPa, the quadrupole and magnetic couplings are comparable. At 18 GPa (b) a magnetically split component (LP2) composed of a familiar pure magnetic-split sextet appears, signaling the quenching of the orbital term. At 20 GPa (c) a *nonmagnetic* third component (HP) appears with substantially lower QS and IS values. At  $P > 32$  GPa (g), HP becomes the only remaining component. LP1 and LP2 both disappear in the intermediate pressure regime [(d)–(f)]. The lines through the experimental points are theoretical curves obtained from the least-squares fitting programs.

Near 18 GPa we detect a second Mössbauer component with a magnetically-split sextet [Fig. 2(b)] coexisting with the LP1 spectrum. The second component is a case in which  $\mu H_{\text{hf}} \gg e^2 q_{zz} Q/2$ , and the following *spin Hamiltonian* applies:

$$H(I^*) = \mu^*(I_z/I^*)H_{\text{hf}} + \{e^2 q_{zz} Q(3 \cos^2 \theta - 1) / [8I^*(2I^* - 1)]\} \{3I_z^2 - I^*(I^* - 1)\} \\ H(I) = \mu(I_z/I)H_{\text{hf}}. \quad (2)$$

The solid line through the experimental points of the second component is the theoretical fit based on Eq. (2), and

results in characteristic MS parameters (at  $\sim 5$  K) of  $H_{\text{hf}} = 32$  T, the quadrupole term  $e^2 q_{zz} Q(3 \cos^2 \theta - 1) = 0$ , and the IS is  $+0.7$  mm/s. The hyperfine field of this phase is substantially larger, and the reason for this large change will be clarified later; however, note that the IS barely changes. The fact that the quadrupole term is zero at  $T < T_N$  is due to realignment of the moments with respect to  $e q_{zz}$ , namely,  $\theta \sim 55^\circ$  where  $(3 \cos^2 \theta - 1) = 0$ .

A third, *nonmagnetic* component, that coexists with the preceding components, is observed upon a minor pressure increase from 18 to  $\sim 20$  GPa [see Fig. 2(c)]. At 23 GPa the LP1 component vanishes, and the abundance of the third component (a nonmagnetic doublet) increases to become easily visible in the central region of the spectrum [Fig. 2(d)]. At 30 GPa [Fig. 2(f)] the nonmagnetic component is dominant, and finally at 40 GPa and beyond, the Mössbauer spectra reflect a single, quadrupole-split component [Fig. 2(g)]. The pressure-dependencies of the parameters obtained from the Mössbauer spectra analyses and of  $T_N$  (Ref. 20) are shown in Fig. 3. The relative abundance of the three components as a function of pressure is shown in Fig. 3(a). The abundance of site  $i$  was determined from the relative areas  $A_i$  under the absorption peaks of each component using the relation  $A_i = K n_i f_i$  where  $n_i$  is the abundance of component  $i$ , and  $f_i$  is its recoil-free fraction.<sup>21</sup>

Up to  $\sim 17$  GPa, where the spectral features of the first (LP1) component in the MS spectra prevail, the following continuous changes are observed with rising pressure: (i)  $T_N$  increases 16-fold to 150 K; (ii)  $H_{\text{hf}}$  increases from 7 to 13 T; (iii) the QS increases monotonically from 0.65 mm/s to a peak of 0.85 mm/s at  $\sim 12$  GPa, followed by a decrease to 0.75 mm/s at  $\sim 18$  GPa; and (iv) the IS decreases almost linearly, from 1.0 to 0.83 mm/s.

At 18 GPa the abundance of LP1 declines to  $\sim 75\%$ , and a magnetic component appears with a considerably larger  $H_{\text{hf}}$  ( $=32$  T) and  $T_N$  ( $=260$  K), albeit with comparable QS and IS values; this component is governed by the *spin-Hamiltonian* expressed in Eq. (2). Since the IS and QS are unchanged, implying the same local electron density and symmetry surrounding the Fe ion, we assign this component to the low-pressure phase and call it LP2. Mössbauer spectra recorded at 18 GPa at various temperatures are shown in Fig. 4, and clearly demonstrate the enhanced values of  $H_{\text{hf}}$  and  $T_N$  associated with LP2. At 20 GPa a nonmagnetic third component with  $\sim 10\%$  abundance appears, while each of the magnetic components contribute  $\sim 45\%$ . This is the highest pressure at which LP1 is still present. The abundance of LP2 peaks at 23 GPa (67%), and then sluggishly decreases to vanish at  $\sim 40$  GPa. The IS and QS values of the LP phases decrease monotonically, yet those corresponding to the *nonmagnetic* component phase barely change to 45 GPa, the highest pressure reached with the MS studies. The reason for the abrupt decrease in IS, i.e., increase in  $\rho_s(0)$  of this HP component, is due to the abrupt decrease in volume following the first-order phase transition.

## B. XRD results

The equation of state  $V(P)$  of  $\text{FeI}_2$ , at 300 K is shown in Fig. 5. The first diffraction lines attributed to the HP phase

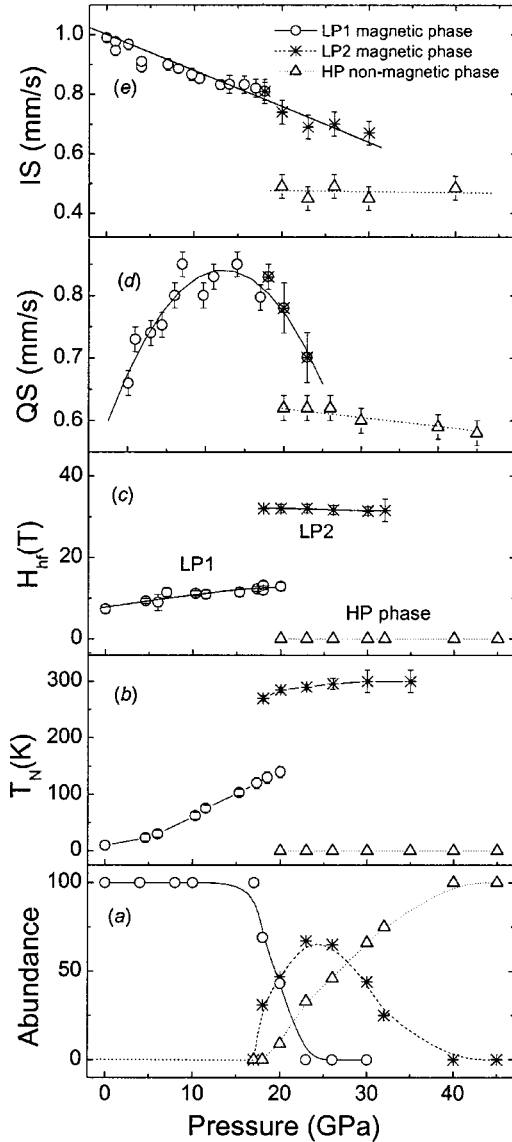


FIG. 3. (a) The pressure evolution of the relative abundance of the MS components as computed from the relative values of the absorption areas (see the text). (b) Pressure dependence of  $T_N$ . Note the abrupt increase in its value at the onset of the LP1→LP2 transition at  $\sim 18$  GPa. (c) Pressure dependence of  $H_{\text{hf}}$ . Up to 18 GPa,  $H_{\text{hf}}$  is the sum of *spin* and *orbit* terms (see the text), but following the orbital quenching at 18 GPa  $H_{\text{hf}}=H_S$ . (d) Pressure dependence of the quadrupole splitting. (e) Pressure dependence of the IS at 300 K relative to a  $^{57}\text{Co}$  (Rh) source at 300 K. All lines are to guide the eye.

were detected at 20 GPa.<sup>22</sup> As can be seen, the  $V(P)$  curves also indicate a coexistence of phases in the 20–30 GPa range, consistent with the MS data [Fig. 3(a)]. Analysis of the HP phase suggests the same  $\text{CdI}_2$ -type layered structure assignment as that of the LP phase with practically the same  $a$  parameter but with a considerably reduced  $c$  parameter (Fig. 5). This suggests that a considerable reduction takes place in the Fe-I interatomic distances following the phase transition.

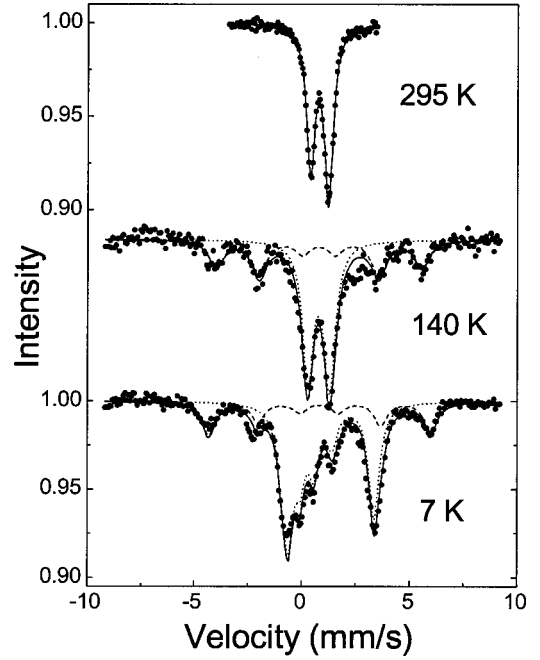


FIG. 4. Mössbauer spectra of the LP orbital-unquenched (LP1) and orbital-quenched (LP2) phases recorded at 18 GPa. At 7 K both components are magnetically ordered; at 140 K the quadrupole-split component corresponding to the paramagnetic LP1 ( $T_N < 140$  K) and the antiferromagnetic LP2 ( $T_N > 140$  K) components are shown, and at 298 K both LP2 and LP1 components are paramagnetic. The fact that the QS and IS at 298 K of the two components are identical, suggests that the LP1→LP2 transition originates from identical chemical and structural Fe local environments.

### C. Electrical resistance results

The pressure dependence of the  $\text{FeI}_2$  resistance measured at 300 K is shown in the inset of Fig. 6. In the 7–25 GPa range the resistance  $R$  decreases by eight orders of magnitude and  $\log R(P)$  drops off to become pressure independent above 20 GPa. The onset of metallization is clearly seen in Fig. 6. At 23 GPa  $\text{FeI}_2$  behaves like a small-band-gap semiconductor but, in fact, is a mixed metal-insulator phase. At 28 GPa and beyond, it clearly shows metallic behavior (positive  $dR/dT$ ) for the major part of the temperature range.

## IV. DISCUSSION

Despite the hexagonal elementary cell, the iodide ions almost form an octahedrons surrounding the Fe ion, thus justifying the presence of an octahedral crystal field (CF). This octahedron surrounding in the hexagonal unit cell can be easily distorted along the local cube diagonal, which lies along the  $c$  axis. This distortion can be assigned as the *trigonal* distortion of the octahedral CF. Reduction and removal of this distortion in this layered compound can be easily achieved through external pressure because of the (preferential) compression of the soft  $c$  axis.

Up to  $P < 18$  GPa the  $\text{Fe}^{2+}$  ( $d^6, \langle S \rangle = 2, \langle L_z \rangle \neq 0$ ) magnetic moment contributes to its hyperfine field through two main terms<sup>23</sup>

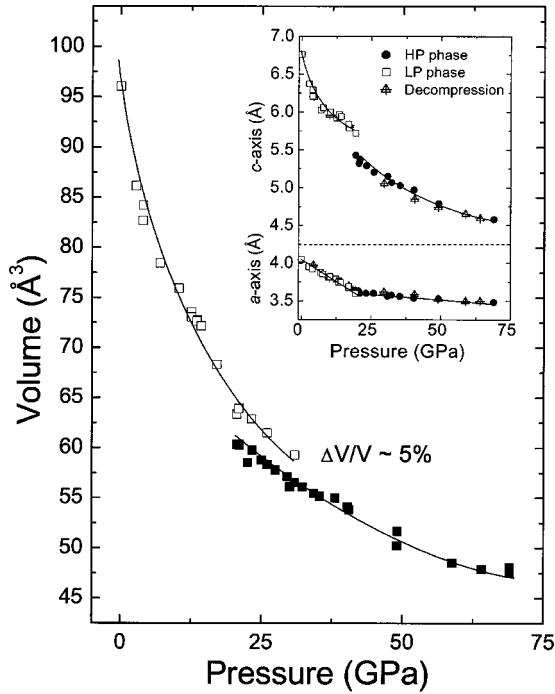


FIG. 5. The equation of state of  $\text{FeI}_2$ . Note the abrupt drop in volume following the first-order transition and the HP-LP coexistence in the 20–31-GPa range. The inset shows the pressure dependence of the hexagonal  $c$  and  $a$  axes.

$$H_{\text{hf}} = H_S + H_O, \quad (3)$$

where  $H_S$  is the *spin term* proportional to  $\langle S \rangle$ ,  $H_O$  is the *orbital term* proportional to  $\langle r^{-3} \rangle \langle L_z \rangle$ . A typical value of  $H_S(\text{Fe}^{2+})$  is  $-30$  T and as was shown in the case of  $\text{FeO}^{24}$   $H_S(\text{Fe}^{2+})$

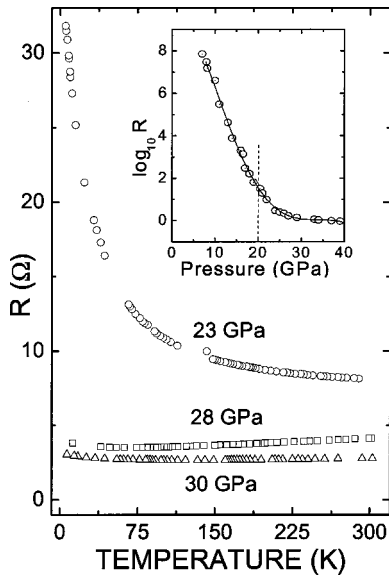


FIG. 6. Electrical  $R(P, T)$  of  $\text{FeI}_2$ . The temperature dependence of the percolative like resistance at 23 GPa reflects the mixed metallic HP and insulating LP phases. Pure metallic behavior is evident at 28 and 30 GPa. The inset shows the pressure dependence of the resistance at 300 K. Note the sharp continuous eight order decrease in  $R$  from 5 to 30 GPa.

barely changes with pressure. In the present case in the 0–18-GPa range,  $|H_{\text{hf}}|$  increases continuously from 8 to 12 T suggesting that the volume dependence of the  $H_O$  term is quite dominant. Considering the unusually small value of  $|H_{\text{hf}}|$  and the fact that  $\partial H_{\text{hf}}/\partial P > 0$ , it can be concluded that:  $H_S$  and  $H_O$  have *opposite signs*, that  $H_O$  due to the  $\langle r^{-3} \rangle$  term is responsible for the *continuous enhancement* of  $|H_{\text{hf}}|$  in the 0–18-GPa range, from 8 to 12 T, and finally because  $H_S(P)$  is constant and negative one concludes that (i)  $H_O$  is *positive* and (ii)  $|H_O| > |H_S|$ , hence (iii)  $H_{\text{hf}} > 0$ .

At 18 GPa, preceding the first-order transition at  $P \sim 20$  GPa, remarkable discontinuous changes in  $H_{\text{hf}}$  and  $T_N$  are observed [Figs. 3(a) and 3(b)]. The hyperfine field jumps from 10 to 30 T, remaining constant with further pressure increase, and  $T_N$  increases from 150 to 260 K at 18 GPa reaching 300 K at 30 GPa, the highest pressure at which the magnetic state is still present. The discontinuous increase in  $H_{\text{hf}}$  (and in  $T_N$ ) can be explained as due to the collapse of the orbital term  $H_O$  due to orbital quenching (OQ), namely,  $\langle L_z \rangle = 0$ , resulting from the significant increase in the CF splitting<sup>25</sup> within the  ${}^5T_{2g}$  low-lying levels manifold. Following the OQ the only term remaining in Eq. (3) is the *spin term*  $H_S$ , which drives  $|H_{\text{hf}}|$  to 30 T, typical of an  $\text{Fe}^{2+}$  ( $d^6, \langle S \rangle = 2, \langle L_z \rangle = 0$ ) configuration. The consequences of the orbital term quenching are (i) a significant increase of the ferrous ion moment; (ii) a drastic increase of  $T_N$ , probably due to increase of the super-exchange interaction; (iii) a reorientation of the magnetic moment with respect to the  $c$  axis; and (iv) possible structural effects.<sup>26</sup> The reorientation of the moments with respect to the  $c$  axis from  $0^\circ$  (and  $180^\circ$ ) in the LP1 regime to  $55^\circ$  (and  $235^\circ$ ) in the LP2 regime<sup>27</sup> is deduced from the combined magnetic/quadrupole spectra (Figs. 2 and 4) and Eq. (2). The least-squares fit to the experimental data showed that  $e^2 q_{zz} Q (3 \cos^2 \theta - 1) = 0$ , and since the QS is not equal to 0 (see Fig. 4), we conclude that  $\cos \theta = \sqrt{1/3}$  or  $\theta = 55^\circ$ .<sup>26</sup> This yields the arrangement of the moments for the LP2 phase pictured in Fig. 1. Note that both the volume and IS do not show any discontinuous change as a result of orbital quenching [Figs. 3(e) and 5(a)] suggesting that this phase transition is second order. We believe that this is the first time that pressure-induced OQ has been reported. The abrupt LP1  $\rightarrow$  LP2 transition probably comes about from a discontinuous increase in the *crystal field*.

*Collapse of magnetism:* At  $P \geq 20$  GPa, one clearly observes (Fig. 2) the presence of a *nonmagnetic* Mössbauer component present at 5 K, the lowest temperature used in this study. It is characterized by a *considerably* smaller IS ( $\sim 0.58$  mm/s) and QS (0.6 mm/s). The fact that  $H_{\text{hf}} = 0$  down to at least 5 K suggests that the HP phase of  $\text{FeI}_2$  is diamagnetic. Diamagnetism in  $\text{Fe}^{2+}$  can result from either (i) a high-spin to low-spin transition ( ${}^5T_{2g} \rightarrow {}^1A_{1g}$ ) in which the six  $d$  electrons are paired, or (ii) a correlation breakdown (a *Mott* or a charge-transfer<sup>28</sup> transition) in which the moments vanish.

Either process may cause a considerable decrease in the  $\text{Fe}^{2+}$  ionic radius, hence in volume, and indeed, it is suggested that the Fe-I nearest-neighbor distance drops discontinuously at the phase transition as intimated from the sharp

drop in the  $c$ -axis lattice constant shown in Fig. 5. The electrical-transport measurements serve to resolve this uncertainty. As shown in the inset of Fig. 6, following the phase transition onset at 20 GPa, a sluggish insulator-metal transition takes place, as evidenced by the leveling-off of the  $R(P)$  curve at  $P > 25$  GPa. The  $R(T)$  curve at  $P = 23$  GPa behaves qualitatively as a gapped state with  $dR/dT < 0$ ; however, a more extensive explanation for this temperature behavior, that is also consistent with the MS findings, is the coexistence of the insulating LP phase with metallic HP phases. Clusters in which the relative abundance of the latter increase with pressure [see Fig. 3(a)] and percolation could account qualitatively for the  $R(P, T)$  conductivity. As the pressure is raised the abundance of the metallic phase increases, reaching 100% at  $P > 30$  GPa. Even at 28 GPa with  $\sim 70\%$  abundance, the HP metallic phase dominates, and its

$R(T)$  plot strongly supports metallization down to 70 K. Therefore, we conclude that the picture of the charge delocalization-metallization process is caused by the I  $5p$ -band overlap with the Fe- $3d$  upper Hubbard (empty) band or by the  $d$ - $d$  band overlap, and concurs with the discontinuous reduction volume, the increase in  $\rho_s(0)$ , and the onset of metallization.

#### ACKNOWLEDGMENTS

This research was supported in part by a LANL-UC IGPP Program Grant No. 919R, by BSF Grant No. 9800003, and by Israeli Science Foundation Grant No. 1998003. We are grateful to Dr. L. Dubrovinsky for his useful comments regarding the XRD analyses, and to the personnel of the ID30 beam in ESRF for their assistance.

\*Also at Los Alamos National Laboratory.

- <sup>1</sup>N. F. Mott, *Metal-Insulator Transitions* (Taylor and Francis, London, 1990), and references therein.
- <sup>2</sup>M. P. Pasternak, R. D. Taylor, A. Chen, C. Meade, L. M. Falicov, A. Giesekus, R. Jeanloz, and P. Y. Yu, *Phys. Rev. Lett.* **65**, 790 (1990).
- <sup>3</sup>M. P. Pasternak, R. D. Taylor, and R. Jeanloz, *J. Appl. Phys.* **70**, 5956 (1991).
- <sup>4</sup>M. P. Pasternak and R. D. Taylor, in *Mössbauer Spectroscopy Applied to Magnetism and Materials Science*, edited by Gary Long and Fernande Grandjean (Plenum, New York, 1996), Vol. 2, Chap. 8, p. 167.
- <sup>5</sup>A. R. Fert, J. Gelard, and P. Carrarea, *Solid State Commun.* **13**, 1219 (1973).
- <sup>6</sup>R. W. G. Wyckoff, *Crystal Structures* (Interscience, New York, 1981), Vol. 1, p. 266.
- <sup>7</sup>J. Gelard, A. R. Fert, P. Mereiel, and V. Allain, *Solid State Commun.* **14**, 187 (1974).
- <sup>8</sup>R. Alben, *J. Phys. Soc. Jpn.* **26**, 261 (1969).
- <sup>9</sup>T. Fujita, A. Ito, and K. Ono, *J. Phys. Soc. Jpn.* **27**, 1143 (1969).
- <sup>10</sup>J. Kanamori, *Prog. Theor. Phys.* **20**, 890 (1958).
- <sup>11</sup>T. Fujita, A. Ito, and K. Ono, *J. Phys. Soc. Jpn.* **21**, 1734 (1966).
- <sup>12</sup>G. R. Hearne, E. Sterer, M. P. Pasternak, and R. D. Taylor, *Hyperfine Interact.* **90**, 447 (1994).
- <sup>13</sup>E. Sterer, Ph.D dissertation, Tel Aviv University, 1992.
- <sup>14</sup>Pure elemental  $I_2$  was prepared by thermal dissociation at 300 °C of spectroscopically pure  $PdI_2$  and condensation of  $I_2$  vapor in the same evacuated tube.
- <sup>15</sup>E. Sterer, M. P. Pasternak, and R. D. Taylor, *Rev. Sci. Instrum.* **61**, 1117 (1990).
- <sup>16</sup>A. Jayaraman, *Rev. Mod. Phys.* **55**, 65 (1983).
- <sup>17</sup>A. P. Hammersley, S. O. Svensson, M. Hanfland, A. N. Fitch, and

D. Hausermann, *High Press. Res.* **14**, 235 (1996).

- <sup>18</sup>A. C. Larson and R. B. Von Dreele (unpublished).
- <sup>19</sup>The quadrupole splitting QS is half the value of the quadrupole coupling  $e^2q_{zz}Q$ .
- <sup>20</sup>Values of  $T_N$  at consecutive pressures were determined by extrapolating  $H_{hf}(T)$  to 0.
- <sup>21</sup>We assumed as a first approximation that at each pressure the recoil-free fraction values  $f_i$  for the three components are the same at 5 K.
- <sup>22</sup>A detailed report of the XRD data of both  $FeI_2$  and isomorphous  $FeCl_2$ , including structural properties of the LP2, phase will be published elsewhere.
- <sup>23</sup>The *intra-atomic dipolar*  $H_{dip}$  term is neglected, based on  $FeCl_2$  data [K. Ono and A. Ito, *J. Phys. Soc. Jpn.* **19**, 899 (1964)] which derived a value of 2.4 T.
- <sup>24</sup>M. P. Pasternak, R. D. Taylor, R. Jeanloz, X. Li, J. H. Nguyen, and C. A. McCammon, *Phys. Rev. Lett.* **79**, 5046 (1997).
- <sup>25</sup>It is of note that the CF splitting increases proportional to the inverse of the fifth power of the TM ligand-bond length [D. M. Sherman in *Advances in Physical Geochemistry*, edited by S. K. Saxena (Springer-Verlag, Berlin, 1988), Vol. 7, p. 113].
- <sup>26</sup>Preliminary XRD data suggest a quite interesting relationship between structure and the onset of OQ in the coexistence pressure range (18–30 GPa) [Rozenberg *et al.* (unpublished)].
- <sup>27</sup>It is worth noting that in the structurally analogous  $NiI_2$  and  $CoI_2$  the angle formed between the  $c$ -axis and the magnetic moment is  $55^\circ$  at ambient pressure, and remains so with increasing pressure up to the collapse of the magnetic state [M. P. Pasternak, G. R. Hearne, E. Sterer, R. D. Taylor, and R. Jeanloz, in *High-Pressure Science and Technology*, edited by S. C. Schmidt, J. W. Shaner, G. A. Samara, and M. Ross (AIP, New York, 1994), p. 335].
- <sup>28</sup>G. Zaanen, G. A. Sawatzky, and J. W. Allen, *Phys. Rev. Lett.* **55**, 418 (1985).